TEM comparison of chrysotile (asbestos) nanotubes and carbon nanotubes

L. E. MURR, K. F. SOTO
Department of Metallurgical and Materials Engineering, The University of Texas at El Paso, El Paso, TX 79968, USA

Fibrous materials, both natural and synthetic, have been an important part of global technologies for decades. Many of these materials in their elemental forms are nanomaterials with unusual properties, especially crystalline whiskers and fibers used to make an array of composite materials systems. Around 1970, asbestos, especially chrysotile ($Mg_3Si_2O_5(OH)_4$), and crocidolite ($Na_2(Fe_3^{2+}, Fe_2^{3+})Si_8O_{22}(OH,F)_2$) had been used to fabricate nearly 80 000 miles of asbestos–cement (AC) water pipe in the United States, alone, hundreds of millions of tons of asbestos insulation, brake-linings, AC sheet (commonly referred to as transite), and a host of other commercial products. But by the early 1970s, the health effects of asbestos mining, milling, and manufacturing began to emerge [1–3], and asbestos was observed in beverages and drinking water [4, 5]. This of course led to a moratorium on AC pipe and other asbestos products, including brake-linings, especially in the United States. Other studies of ingested mineral fibers, including asbestos, suggested that asbestos fibers longer than 20 μm but thinner than 3 μm were more carcinogenic than fibers of greater diameter, regardless of length, or those shorter than 20 μm, regardless of diameter. Of course, these were actually fiber bundles.

It is now well known that the geometry and surface chemistry of particulates can play an important role in causing lung toxicity, especially chrysotile asbestos exposure [6]. Renwick *et al.* [7] have demonstrated that ultrafine particulates impair macrophage phagocytosis to a greater extent than fine particles (compared on a mass basis). Schwartz *et al.* [8] have shown that episodes involving high concentrations of coarse particles are not associated with increased mortality while Oberdörster *et al.* [9] correspondingly showed that ultrafine particles contribute to acute mortality. In addition, crystalline particulates in contrast to amorphous particulates in the same size range are more damaging to human lungs [10], and Momarca *et al.* [11] have shown that ultrafine crystalline particulates are major contributors to adverse health effects. There is mounting evidence that ultrafine airborne particulates with mean diameters $<$100 nm are far more toxic than expected and pose considerable health risks, including mortality, asthma complications, chronic bronchitis, respiratory tract infections, ischaemic heart diseases, and stroke. A recent joint industry, government, and private sector, multicity analysis found that a daily increase of 20 $\mu g/m^3$ in inhalable particulate matter $<$10 μm increased the death rate by about 1% [12], while a 25 $\mu g/m^3$ increase in average lifetime concentration of fine particles ($<$2.5 μm diameter) increased the overall total annual death rate by some 15% [13].

The start of the 21st century heralded the U.S. National Nanotechnology Initiative [14], following a decade of materials discovery and development, notably carbon nanotubes [15], which have demonstrated a wide range of remarkable properties [16]. This has led to predictions of annual production quantities of single-wall carbon nanotubes (SWCNTs) in thousands of tons within the first decade of the 21st century [17]; however, large quantities of multiwall carbon nanotubes (MWCNTs) are already in commercial use [18].

In a recent summary of American Chemical Society Symposium on Nanomaterials and Nanotechnology, Dagani [19] concluded that "early results suggest that some nanoparticles, such as carbon nanotubes, may pose health risks." Correspondingly, Lam *et al.* [20] have recently shown that SWCNTs are more toxic than carbon black or silica (SiO_2) particulates (on an equal weight basis) in mouse lungs, while Warheit *et al.* [21] have demonstrated that pulmonary exposures to SWCNTs in rats produced evidence of a foreign tissue body reaction. Recent exposure assessment studies conducted at workplace sites where carbon nanotubes are either manufactured or utilized reported low airborne particulate exposure levels of respirable SWCNTs, not exceeding 100 $\mu g/m^3$ [22, 23]. Moreover, it has recently been observed that carbon nanotubes, particularly MWCNTs are ubiquitous in the atmosphere, both indoor and outdoor, and are produced by a wide range of fuel gas combustion sources, including natural gas and propane gas kitchen stove tops, gas furnaces and hot water heaters, electric power generation stations, etc. [24–26]. These airborne MWCNT particulates are actually complex aggregates often composed of hundreds or thousands of carbon nanotubes and related carbon nanocrystal particles. While specific quantitation has not been measured, estimates of carbon nanocrystal aggregate concentrations can exceed 100 $\mu g/m^3$.

While the technological and health-related issues involving carbon nanotubes have emphasized SWCNTs, it is apparent that the most prevalent occurrence of carbon nanotubes is MWCNTs and especially complex aggregates of MWCNTs and related carbon nanocrystal forms. Harris [27] has noted that chrysotile

0022–2461

asbestos is strikingly similar to carbon nanotubes, particularly MWCNTs. Consequently, considering the pervasive health consequences of asbestos, studies and comparisons of MWCNTs and chrysotile nanotubes (or their aggregates) may be especially enlightening. This study illustrates striking similarities between combustion-formed, multiwall carbon nanotubes and natural chrysotile asbestos nanotubes through observations in the transmission electron microscope (TEM).

Fibers from a chrysotile mineral specimen from Quebec Province, Canada were placed in a sandwich of two carbon/formvar-coated Ni mesh TEM grids and examined in the TEM: a Hitachi H-8000 analytical TEM fitted with a Noran energy-dispersive (X-ray) spectrometer (EDS) system and a goniometer-tilt stage, operated at 200 kV accelerating potential. Samples of multiwall carbon nanotubes and related carbon nanocrystal aggregates were collected from the exhaust streams of propane and natural gas kitchen stove top burners by thermal precipitation onto single carbon/formvar or silicon monoxide/formvar-coated Ni or Cu mesh TEM grids. The thermal precipitation device utilizes a heated wire to produce a thermal gradient relative to an ice-water-cooled copper block onto which the TEM grid substrates were placed, causing airborne particle adsorption to produce a corresponding collection efficiency of about 90%, described previously by Bang *et al.* [28].

Fig. 1 shows typical examples of MWCNT aggregates collected from a propane gas kitchen stove top burner exhaust. The lower magnification TEM image in Fig. 1a shows a complex aggregation of longer MWCNTs and various other concentric graphene (carbon sheet) nanocrystals or quasicrystal forms. Note that these carbon nanoforms exhibit end caps. These features are more readily observable in the more magnified example shown in Fig. 1b. The random arrangement of varying sizes and types of concentric, closed, graphene shells and more elongated concentric (multilayer) graphene, closed tubes gives rise to a very fine, nanocrystal, ring diffraction pattern which is shown in the insert in Fig. 1a. Prominent graphite (hexagonal: $a = 0.25$ nm; $c = 0.67$ nm) reflections are indicated, and correspond to interplanar crystal or d-spacings ($d = \lambda L/R$, $\lambda L =$ camera constant in Å cm when the diffraction ring radii are measured in cm) of 0.34 nm and 0.21 nm for (002) and (100) respectively. It can be noted in Fig. 1b that the tube core diameter varies from roughly 3 nm to 5 nm while the outer tube diameters vary from 5 nm to 15 nm. Similar features are exhibited for natural gas (~96% methane) kitchen stove burner-derived carbon nanocrystal aggregates shown typically in Fig. 2. The selected-area electron diffraction (SAED) pattern insert in Fig. 2a illustrates a higher degree of crystallinity or larger graphene crystal domains because the corresponding (002) diffraction ring is composed of regular diffraction spots. The MWCNTs shown in the enlarged view of Fig. 2b also show capped nanotubes with an internal core diameter of 5 nm and outer tube diameters ranging from ~10 nm to 15 nm.

Fig. 3 shows, for comparison with Figs 1 and 2, typical TEM images of chrysotile asbestos nanotubes which also occur in fibril aggregates, but with a propensity of long nanotubes. As indicated by the corresponding arrows in Fig. 3a and b, these nanotubes are predominantly capped. Like the MWCNTs in Figs 1b and 2b the chrysotile nanotubes in Fig 3b have a core diameter of 5 nm while the outer tube diameters vary from ~15 nm to 35 nm. The SAED pattern insert in Fig. 3a shows typical diffraction streaks perpendicular to the crystal (monoclinic: $a = 0.53$ nm, $b = 0.91$ nm, $c = 1.46$ nm) axis (c-axis direction); (002) and (004) reflections are indicated corresponding to crystal d-spacings of 0.73 nm and 0.37 nm respectively [29, 30].

It is interesting to note that while the chrysotile nanotubes shown in Fig. 3 are predominantly capped, Harris [27] has asserted that "capped chrysotile tubes are never observed." But Murr and Kloska [5] also observed capped chrysotile tubes in fibril aggregates collected from municipal water supplies, and Fig. 3 therefore demonstrates that MWCNTs and chrysotile nanotubes are more similar than suspected. Of course because chrysotile nanotubes or aggregated fibrils are brittle, the tubes are easily and frequently broken, and these features are illustrated in Fig. 4. In fact in the earlier TEM work by Yada [30] the samples observed were primarily crushed. In contrast to chrysotile, carbon nanotubes, both single wall and multiwall, are not brittle, and may be difficult to break. Consequently if toxicology studies compare chrysotile nanotubes with carbon nanotubes, the propensity of broken, uncapped chrysotile nanotubes may cause cell responses different from capped nanotubes. While the appearance of the multiwall carbon nanotube caps in Figs 1 and 2 and those shown for the chrysotile nanotubes in Fig. 3 look essentially the same, they are likely different, especially because the chrysotile must incorporate a tetrahedral silicate layer and a layer containing Mg coordinated to oxygen to create continuous curvature [31]. In contrast, each concentric carbon nanotube can be capped in a large number of different ways, especially when the tube diameter exceeds about 1 nm [27]. Nonetheless, all capped carbon nanotubes must obey Euler's law: a hexagonal lattice of any size can only form a closed structure by the inclusion of 12 pentagons, or 6 pentagons for a hemisphere equivalent. For example, a single wall nanotube would close with half a C_{60} fullerene (buckyball), while larger tubes in concentric, multiwall carbon nanotubes would require half spheres correspondingly larger than C_{60}.

Of lesser importance in comparing the carbon nanotubes and the chrysotile nanotubes would be the differences in actual tube formation, shown to differ from spiral to concentric layers for both chrysotile [31] and carbon [27] nanotubes, although the propensity of multilayer carbon nanotubes seems to be concentric.

While the issue of capped nanotubes versus broken, uncapped nanotubes may be important in toxicology or related studies incorporating chrysotile in comparison to carbon nanotubes, there is also the question of

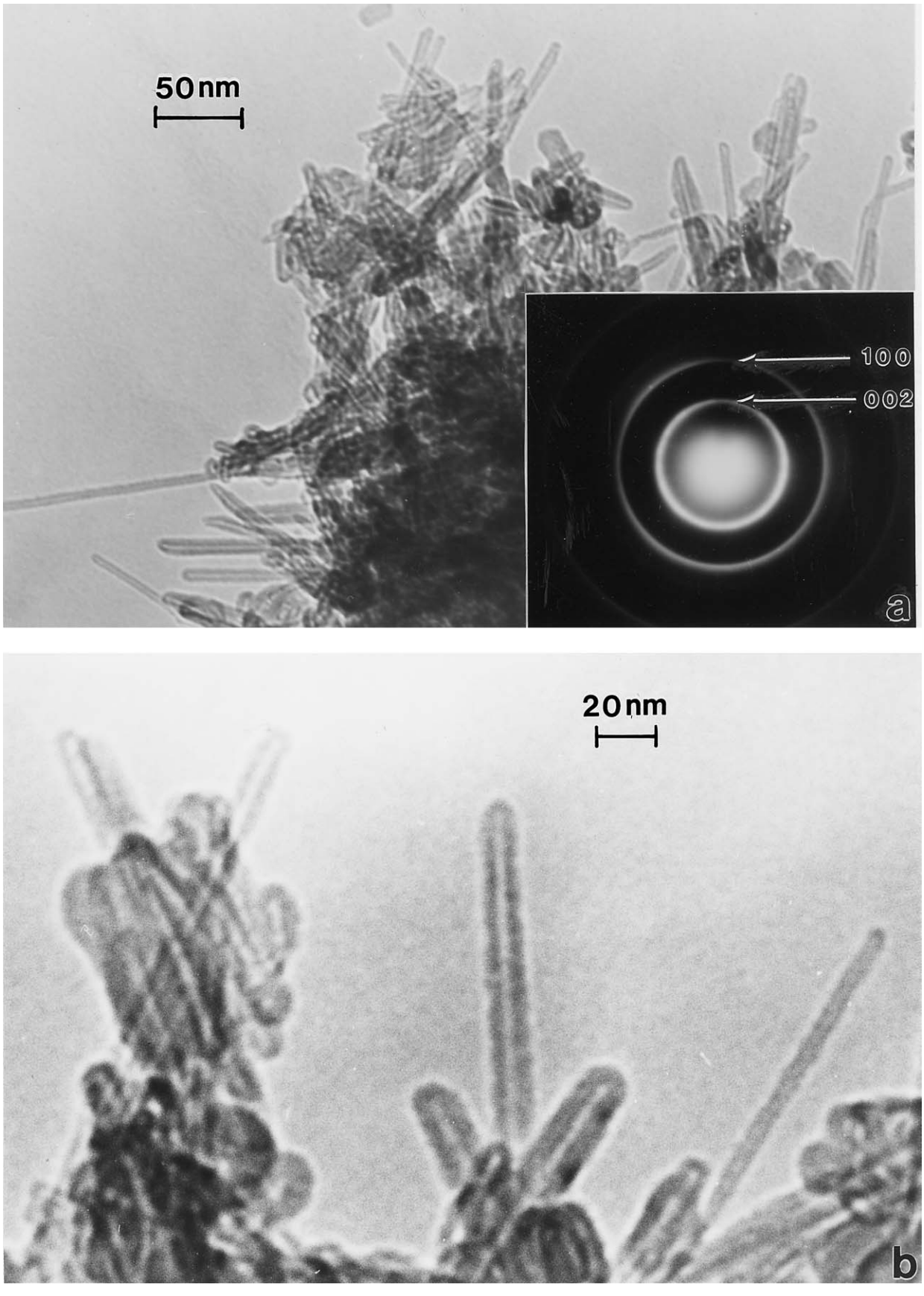

Figure 1 TEM bright-field images of carbon nanotube and related carbon nanocrystal aggregates extracted for a propane gas (propane/air) flame exhaust: (a) portion of carbon particle aggregate showing numerous multiwall nanotubes. Selected-area electron diffraction (SAED) pattern insert shows graphite (002) and (100) diffraction rings and (b) magnified view of multiwall carbon nanotubes at the edge of an aggregate.

actually qualifying the cell exposure to carbon nanotubes since single-wall carbon nanotubes may pose differences from multiwall carbon nanotubes, and the actual propensity of carbon nanotubes amongst other fullerene forms may be an even more serious concern. Indeed, in the recent studies of Warheit *et al.* [21], the experimental particulate regime, characterized as single-wall carbon nanotubes, actually consisted of

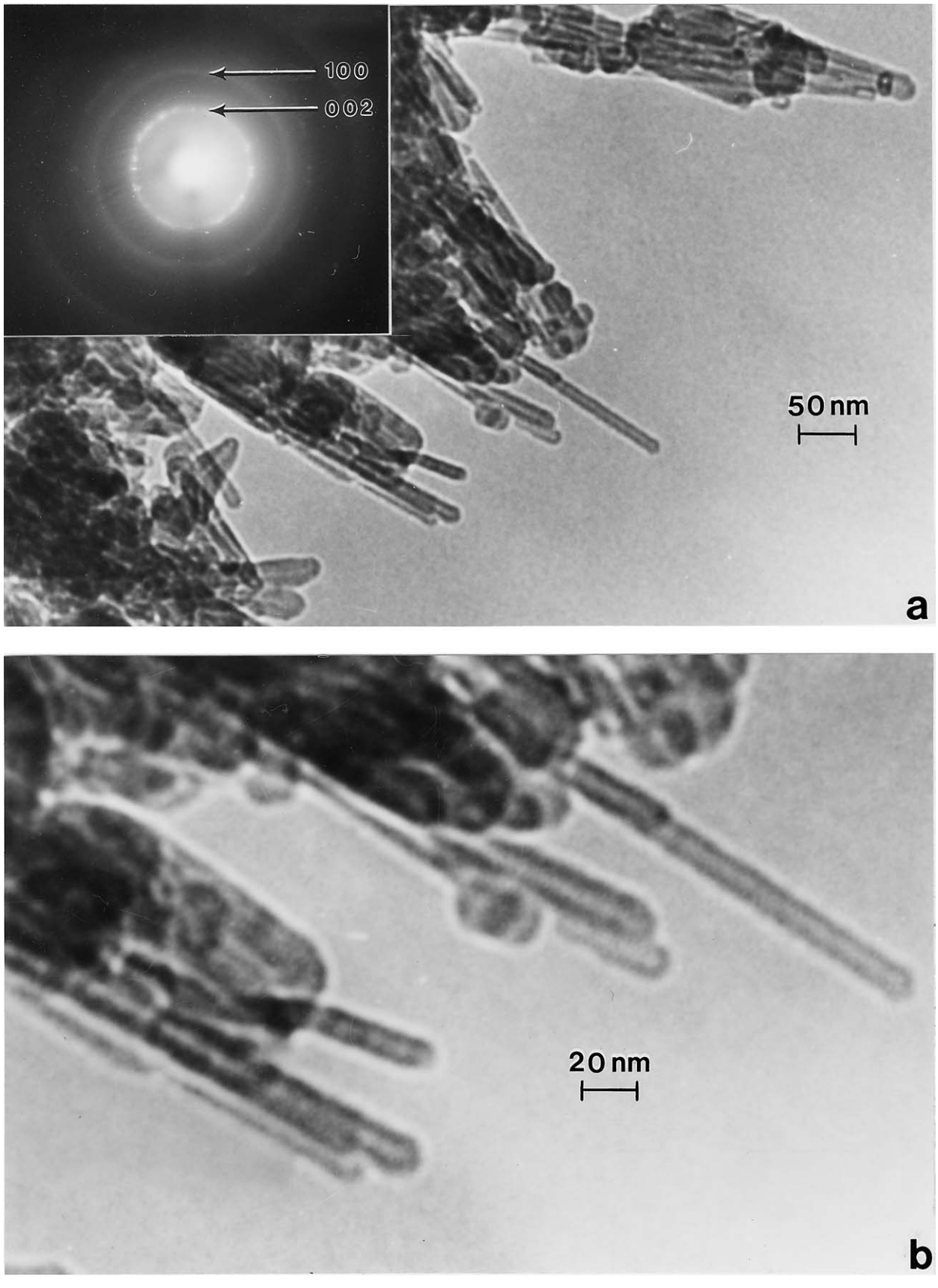

Figure 2 TEM bright-field images of carbon nanotube and related carbon nanocrystal aggregates extracted from a natural gas (natural gas/air) flame exhaust: (a) portion of large carbon particle aggregate showing numerous multiwall nanotubes. SAED pattern insert shows graphite (002) and (100) diffraction rings and (b) magnified view of (a) showing nanotube structures, sizes, and size variations.

laser-ablation generated soot [32] composed of 30–40% (by weight) amorphous carbon, 5% each of Ni and Co, and the balance being carbon nanotube agglomerates, or agglomerated "ropes" or bundles (~30 nm in diameter composed) of individual tubes ~1.4 nm in diameter, roughly one-third the diameter of the smallest tube in Fig. 1b. Consequently, nanomaterials must be carefully characterized in order to differentiate morphology,

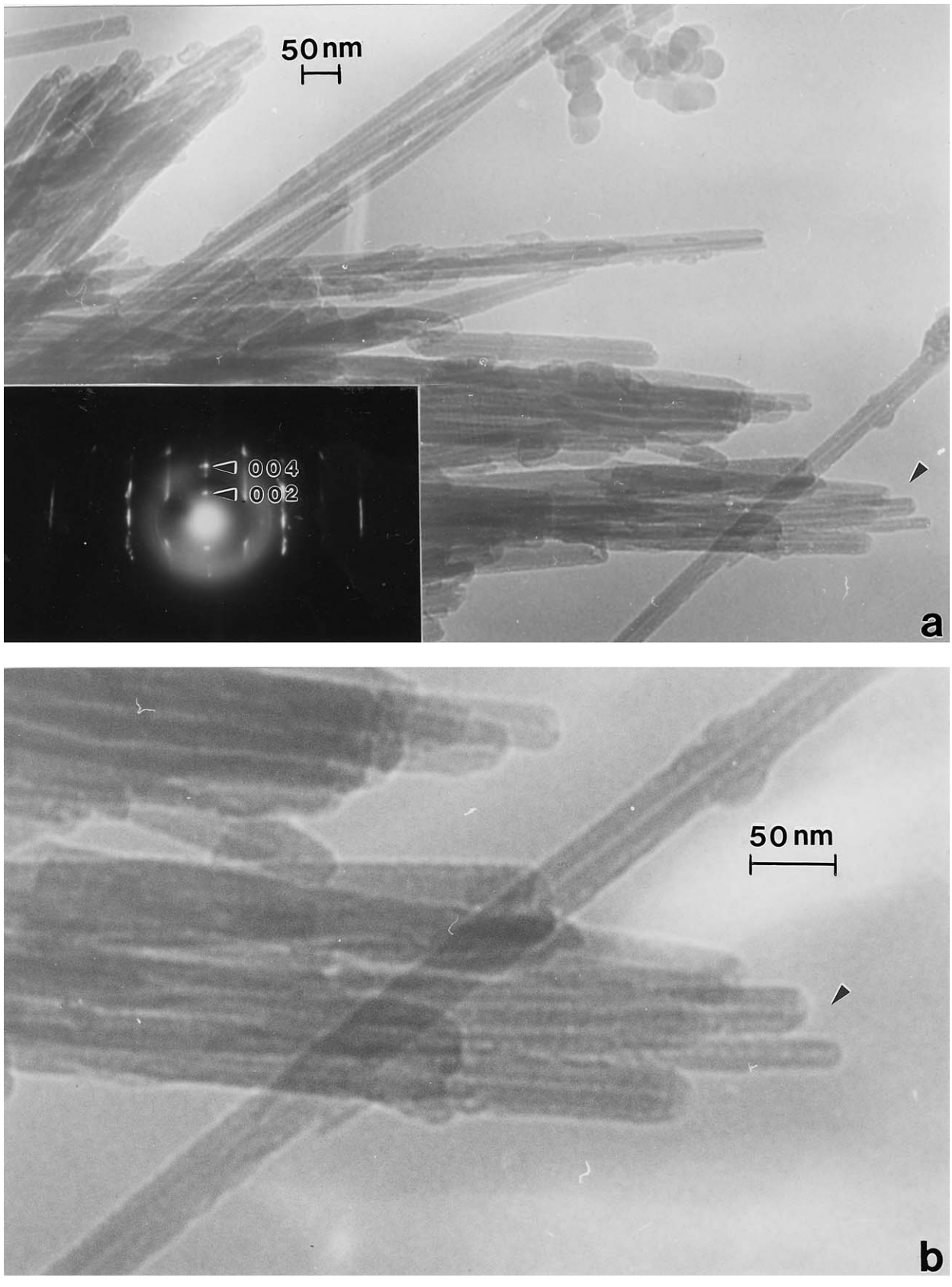

Figure 3 TEM bright-field images of chrysotile asbestos nanotube (fibril) aggregates: (a) typical aggregate portion with corresponding SAED pattern insert showing chrysotile (002) and (004) diffraction spots and (b) magnified view of (a) with emphasis on regions indicated by reference arrows.

size, crystallinity, and chemistry effects. Such characterization must include TEM analysis as illustrated herein.

We have observed end caps or closed nanotubes of both carbon nanotubes and chrysotile asbestos nanotubes by TEM. Multiwall carbon nanotubes and chrysotile asbestos nanotubes are therefore strikingly similar and this should be an important consideration in the evaluation of potential toxicological effects of aggregates of multiwall carbon nanotubes.

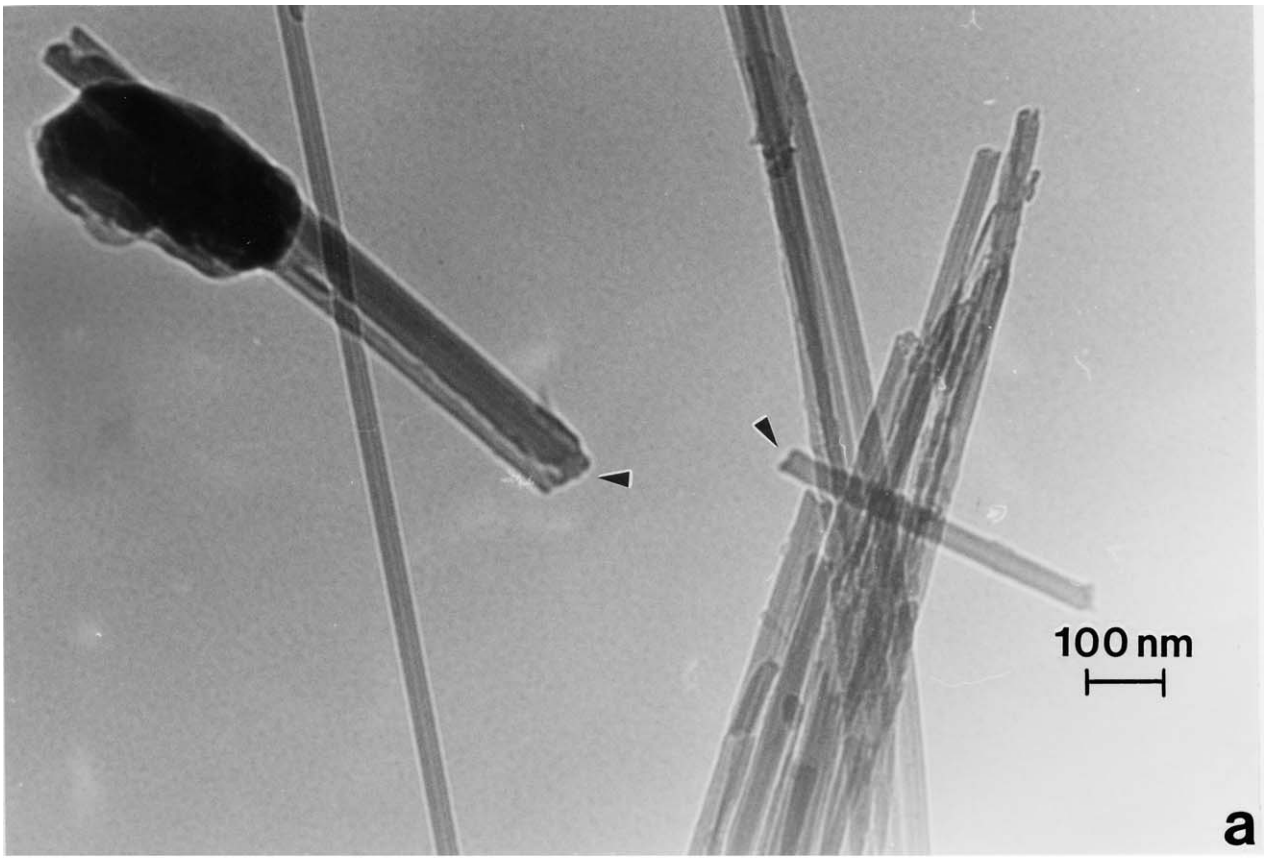

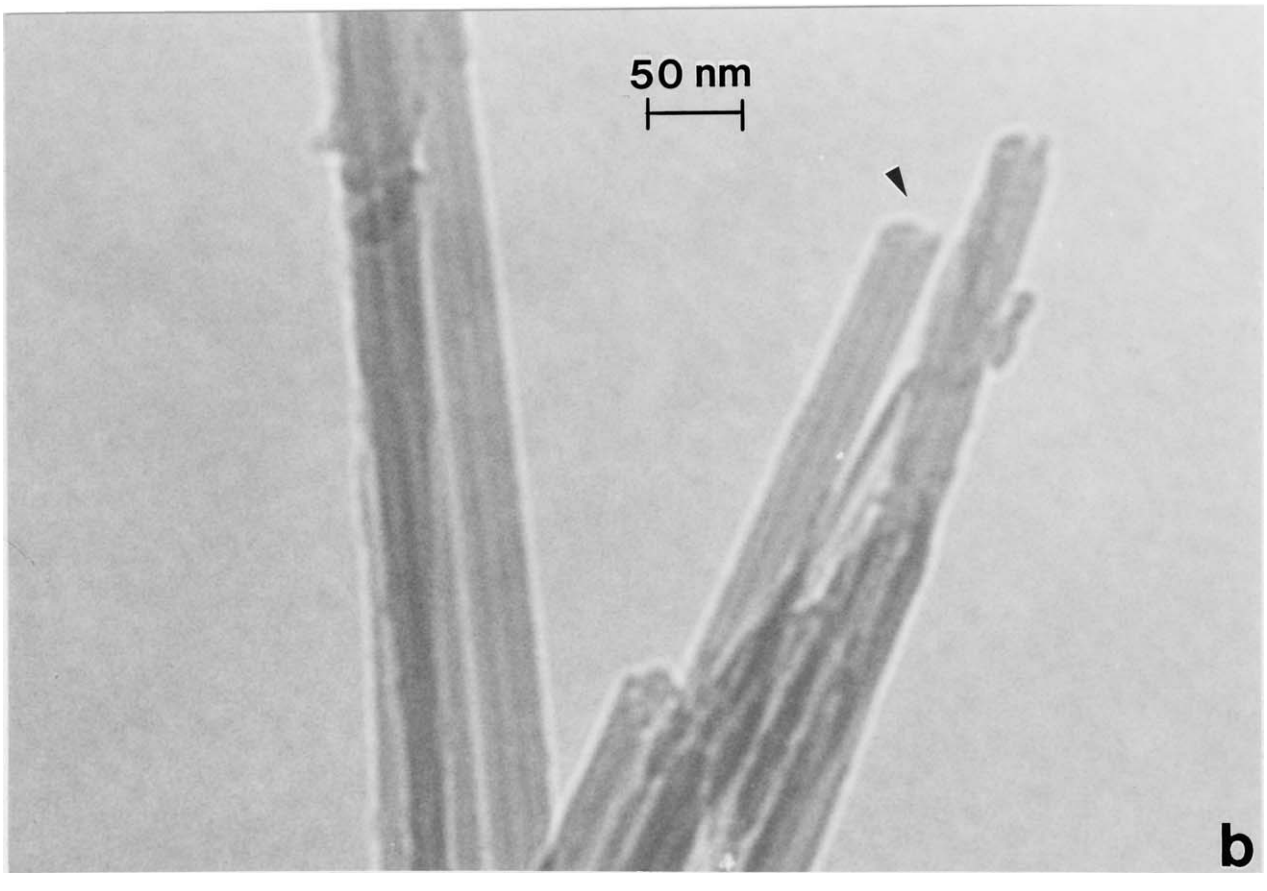

Figure 4 TEM bright-field images of chrysotile asbestos fibrils exhibiting broken segments: (a) and (b) show low and higher magnification sequence referenced to the arrow designated *r*. Other broken ends are indicated by arrows in (a).

Acknowledgments

This research was supported in part by an EPA-Southwest Center for Environmental Research and Policy (SCERP) grant Q00747, project A-02-5, and University of Texas System, Louis Stokes Alliance for Minority Participation (LSAMP) Bridges to Doctorate

Fellowship (KFS). We are grateful to Dr. Phil Goodell of the UTEP Geological Sciences Department for providing the chrysotile mineral specimen.

References

1. J. C. MC DONALD, *Archs. Environ. Health* **22** (1971) 677.
2. P. ENTERLINE, P. DECOUFLE and V. HENDERSON, *J. Occup. Med.* **14** (1972) 897.
3. I. WEBSTER, *Sth. Afr. Med. J.* **47** (1973) 165.
4. H. M. CUNNINGHAM and R. PONTEFRACT, *Nature* **232** (1971) 332.
5. L. E. MURR and K. KLOSKA, *Water Res.* **10** (1976) 469.
6. M. L. LIPPMANN, *Ann. Occup. Hyg.* **38(4)** (1994) 459.
7. L. C. RENWICK, K. DONALDSON and A. COUTER, *Toxicol. Appl. Pharmacol.* **172**(2) (2001) 119.
8. J. SCHWARTZ, G. NORRIS, T. LARSON, L. SHEPPARD, C. CLAIBORNE and J. KOENIG, *Environ. Health Perspect.* **107**(5) (1999) 339.
9. G. OBERDÖRSTER, R. M. GELEIN, J. FERIN and B. WEISS, *Inhal. Toxicol.* **7** (1995) 111.
10. C. J. JOHNSON, K. E. DRISCOLL, J. N. FINKELSTEIN, R. BAGGS, M. A. OREILLY, S. CARTER, R. GELEIN and G. OBERDÖRSTER, *Toxicol. Sci.* **56**(2) (2000) 405.
11. S. MOMARCA, R. CREBELLI, D. TERRETTI, A. ZANARDINI, S. FUSELLI and L. FILINI, *Sci. Total Environ.* **205**(2/3) (1997) 137.
12. J. SAMET *et al.* N., *Engl. J. Med.* **343** (2000) 1742.
13. D. KREWSKI, *et al.*, "Reanalysis of the Harvard Six Cities Study and the American Cancer Society Study of Particulate Air Pollution and Morality: Investigators Report, Part I & Part II" (Health Effects Institute, Boston, MA, 2000).
14. National Nanotechnology Initiative Leading to the Next Industrial Revolution. The White House, Office of the Press Secretary (U.S.A.). 2000: http://clinton4.nara.gov.textonly/WH/New/html/20000121_4.html.
15. S. IIJIMA, *Nature* **354** (1992) 56; *Mater. Sci. Engr.* **B19** (1993) 172.
16. P. M. AJAYAN and T. W. EBBESEN, *Rep. Prog. Phys.* **60** (1997) 1025.
17. P. BALL, *Nature* **414** (2001) 142.
18. H. S. NALWA (ed.), "Handbook of Nanostructural Materials and Nanotechnology" (Academic Press, San Diego, 1999) Vols. 1 & 2.
19. R. DAGANI, *Chem & Engr. News* **81**(17) (2003) 30.
20. C.-W. LAM, J. T. JAMES, R. MCCLESKEY and R. L. HUNTER, *Tox. Sci.* **26** (2003).
21. D. B. WARHEIT, B. R. LAWRENCE, K. L. REED, D. H. ROACH, G. A. M. REYNOLDS and T. R. WEBB, *ibid.* **26** (2003).
22. P. A. BARON, A. D. MAYNARD and M. FOLEY, "Evolution of Aerosol Release During the Handling of Unrefined Single Walled Carbon Nanotube Material," NIOSA Report, NIOSH DART-02-91, December, 2002.
23. A. D. MAYNARD, P. A. BARON, M. FOLEY, A. A. SHVEDOVA, E. R. KISINE and V. CATRANOVA, "Exposure to Carbon Nanotube Material 1: Aerosol Release During the Handling of Unrefined Single Walled Carbon Nanotube Materials," to be published.
24. L. E. MURR, J. J. BANG, D. A. LOPEZ, P. A. GUERRERO, E. V. ESQUIVEL, A. R. CHOUDHURI, M. SUBRAMANYA, M. MORANDI and A. HOLIAN, *J. Mater. Sci. Letters* (2004) in press.
25. J. J. BANG, P. A. GURRERO, D. A. POLEZ, L. E. MURR and E. V. ESQUIVEL, *J. Nanosci. Nanotech.* (2004) in press.
26. L. E. MURR, K. F. SOTO, E. V. ESQUIVEL, J. J. BANG, P. A. GUERRERO, D. A. LOPEZ and D. RAMIREZ, "Carbon Nanotubes and Other Fullerene-Related Nanocrystals in the Environment: A TEM Study, 5th Global Innovations Symposium on Materials Processing and Manufacturing: Surfaces and Interfaces in Nanostructured Materials and Trends in LIGA, Miniaturization, and Nono-Scale Materials," edited by J. Smugeresky and M. Mukhopadhyay (TMS, Warrendale, PA, 2004).
27. P. J. F. HARRIS, "Carbon Nanotubes and Related Structures: New Materials for the Twenty-First Century" (Cambridge, Univ. Press, England, 2003).
28. J. J. BANG, E. A. TRLLO and L. E. MURR, *J. Air and Waste Managemt. Assoc.* **53** (2003) 1.
29. K. YADA, *Acta Cryst.* **23** (1967) 704.
30. *Idem.*, *ibid.* **27** (1971) 659.
31. J. L. HUTCHISON, D. A. JEFFERSON and J. M. THOMAS, *Surf. Defect Prop. Solids* **6** (1977) 320.
32. A. G. RINZLER, J. LIU, H. DAI, P. NIKOLAEV, C. B. HUFFMAN, F. J. RODRIGUEZ-MACIAS, P. J. BOUL, A. H. LU, D. HEYMNAN, D. T. COLBERT, R. S. LEE, J. E. FISCHER, A. M. RAO, P. C. EKLUND and R. E. SMALLEY, *Appl. Phys. A.: Materials Science & Processing* **A67**(1) (1998) 29.

Received 22 January
and accepted 29 March 2004